Control design and experimental validation of an adaptive spindle support for enhanced cutting processes

R. Neugebauer(1), W.-G. Drossel(3), A. Bucht, B. Kranz, K. Pagel

Fraunhofer Institute for Machine Tools and Forming Technology IWU, Chemnitz/Dresden, Germany

In this paper we present an adaptive spindle support that can be used for additional fine positioning movements during machining operations. This is achieved by an overlaid piezo-based hexapod-kinematic structure that is mounted between the machine structure and the motor spindle. Here we present the analysis of the spindle support regarding control aspects. The basis is a finite-element-model that was used to determine a state-space-model of the component. The model was validated by an experimental modal analysis of the structure. Knowing the modal characteristics allows an analysis of the mechanical couplings between the different axes of the spindle support which accordingly enables the design of a controller considering mechanical couplings. For experimental validation the controller was implemented into a rapid prototyping system. The presented results show that during cutting operations the spindle can be moved with high precision within a wide range of frequencies.

Piezo-electric, Control, Adaptive Spindle

1. Introduction

The main challenge in production technology of cutting operations is to increase precision and productivity. A suitable approach to improve productivity is to operate multiple production steps by one machine that is within the same clamping. Therefore, it is necessary to develop machines that on the one hand offer a high chipping volume for pre-finishing production steps and on the other hand guarantee high precision for the finishing production steps. Optimization of existing systems as described in [1] is an appropriate way, but the estimated potential or improvement is rather limited. In contrast, the redesign of whole systems using mechatronic components [2] provides significant improvement.

To overcome this conflict different approaches have been established, with uni-axial approaches [3], [4] being the most relevant. However, the enhancements of complex cutting processes require more than one degree of freedom. Applying uni-axial approaches in multiple axes systems requires increased efforts in the mechanical design. Due to the decreased stiffness of such systems this is often accompanied with limitations in the operating frequency. A multiple axes interface was developed to overcome these problems. The mechanism consists of six piezoceramic actuators in a parallel arrangement. While one end is fastened on the main housing, the other end is connected to a solid state joint that supports a standard HSC-spindle. As shown in Figure 1 there are three pairs of actuators located around the z-designed in a differential configuration. The mechanical design of this component was published in [5]. In comparison to similar solutions [6], this mechanism not only compensates static/dynamic deformations of the tool or damps vibrations, but is also suitable to realize defined deflections of the TCP. That enables the creation of defined surface irregularities during the cutting process.

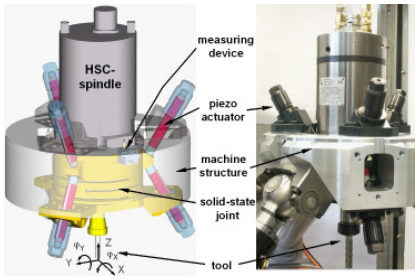

Figure 1: The CAD model of the adaptive spindle support (left) and real component (right) mounted in a Parallel-Kinematic Machine (PKM).

2. Modelling and experimental analysis

2.1. System setup

The central scheme of the adaptive spindle is shown in Figure 2. The vector $\mathbf{Z}_r$ containing values in Cartesian coordinates are derived from the given surface geometry and are set as reference value of the control loop. Due to the configuration of the piezo actuators the reference values have to be transformed into the actuator coordinate system. This can be achieved by multiplying the vector with the Jacobian matrix of the system. The resulting vector contains the necessary displace-

ment of each actuator and represents the reference values for six power amplifiers with a maximum output voltage of 1000V. The spindle position is measured by five capacitive displacement sensors. Considering the geometric positioning of the sensors, the displacement of the Tool-Centre-Point (TCP) in Cartesian coordinates has to be recalculated via sensor transformation.

To realize defined surface geometries it is necessary to implement a position feedback control to the spindle. Therefore, the measured TCP-displacements are compared with the given reference values. The difference between the reference values $\mathbf{Z}_r$ and the actual values $\mathbf{Z}_a$ represent the controller input. The controller calculates an actuating value for each of the Cartesian axes.

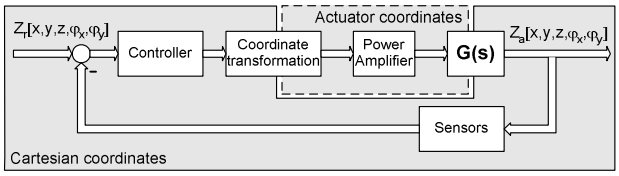

Figure 2: Control scheme of the adaptive spindle support.

The arrangement of the piezoceramic actuators and the stiffness of the solid-state-joint generate couplings between the different axes. A reference displacement in x-direction for example, causes actuation values for all actuators. Therefore, the dynamic behaviour of the system not only depends on the dynamics in the actuated direction, as in serial kinematic machines, but instead depends on the dynamic behaviour in all directions. These couplings have to be considered in the designing process of the controller.

2.2. Finite-element-model

To evaluate the mechanical design and to estimate the performance of the adaptive spindle support, a FE-Model of the component was created. The support used for the experimental investigation of the adaptive spindle was incorporated in the FE-model to represent the boundary conditions realistically. Considering the piezo-ceramic actuators as the dominant stiffness in the system the model not only contains the mechanical properties of the component, but also represents the electro-mechanical behaviour of the actuators. In order to take that into account the simulation method presented in [7] was used. The method considers energy conversion in piezoceramic actuators and expands the model by the electrical parameters of the actuators. To compare the calculated model with the measured data, a modal based state space model was created from the FE-Data. The inputs of the state space model are the charges in the actuators and the forces in x,y,z-direction at the TCP. The relative displacements of the structure at the sensor points were defined as outputs. The model was exported in state-space-form, enabling easy data handling with Matlab. The missing transformations like the conversion from voltage to charge and the sensor transformation were added in Matlab.

2.3. Experimental analysis

Due to the bad accessibility of the solid state joint and the actuators, a complete experimental modal analysis of the adaptive spindle support would require enormous effort. Measurement of the transfer functions from the actuators to the displacement sensors, however, represents a suitable alternative to validate the FE-model.

Figure 3 shows the comparison between measured and calculated data. The Frequency Response Function (FRF) was identified by tilting the spindle around the x-axis. The first eigenfrequencies in the model are close to the measured ones. Therefore, it can be assumed that the calculated eigenforms also meet the real eigenforms. For the control design especially the eigenforms that affect more than one direction are significant. The eigenform at 204Hz for example (Figure 4) has a main deflection in φ_x-direction, but also affects movements in φ_y (see Figure 3) and y-direction. An appropriate way to deal with the couplings is to prevent them by an adequate mechanical design. Due to the cross stiffness of the solid state joint this approach is not always applicable. In such cases the couplings have to be considered in the control design.

To design a decoupling network it is necessary to describe the transfer behaviour of an elastic structure in the frequency domain. These transfer functions can be written in modal parameters as sum of the eigenmodes as shown in equation 1.

$$G_{i,j}(s) = \sum_{r=1}^{n} \frac{\Phi_{ir}\Phi_{jr}}{M_r} \cdot \frac{1}{s^2 + 2\Lambda_r \omega_r s + \omega_r^2} \tag{1}$$

The parameter Φ represents the components of the eigenvector. Λ_r typifies the modal damping, ω_r the eigenfrequency and M_r the modal mass of the r-th eigenmode. $G_{i,j}$ was examined by measuring the transfer functions from all inputs to outputs. The modal parameters can be extracted from the measured results by using appropriate software, like ME'Scope. In this way it is possible to get a numeric model which is based on the physical dependencies of the structure. Comparing the measured transfer functions and the FE-calculations enables the allocation of calculated eigenforms to measured eigenfrequencies.

3. Multiple-axes control concept

3.1. Examining existing couplings

A linear MIMO-System (Multiple Input - Multiple Output) can be described in matrix notation by the input vector **U**, the output vector **Z** and the matrix of the transfer functions **G**. The notation is given in Eq. 2.

$$\mathbf{Z}(s) = \mathbf{G}(s) \cdot \mathbf{U}(s) \tag{2}$$

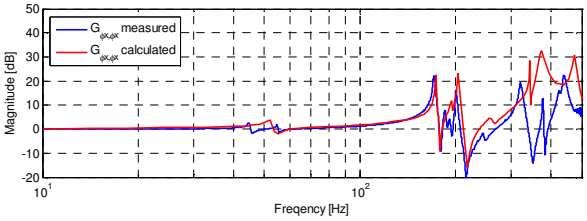

Figure 3: Comparison of the FRF resulting from a reference displacement in φ_x (tilting around x-axis).

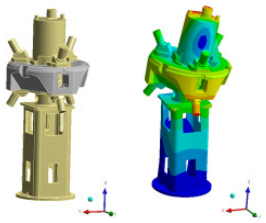

Eigenforms

Nb.	Frequency FE-Model	Frequency measured	Main component
1	52,9 Hz	44,5 Hz	deflection x
2	53,1 Hz	54,7 Hz	deflection y
3	174,1 Hz	171,0 Hz	tilting φ_x,φ_y
4	194,9 Hz	185,3 Hz	tilting φ_y
5	203,8 Hz	201,3 Hz	tilting φ_x
6	259,7 Hz	245,9 Hz	translation z

Figure 4: FE-Model of the spindle support and eigenform of the 5th eigenmode at 204 Hz. (tilting x-axis).

The matrix **G** contains the transfer functions $G_{i,o}$ from input i to output o and has the dimension 5x5 as shown in Eq. 3.

$$\begin{bmatrix} x(s) \\ y(s) \\ z(s) \\ \varphi_x(s) \\ \varphi_y(s) \end{bmatrix} = \begin{bmatrix} G_{x,x}(s) & G_{y,x}(s) & G_{z,x}(s) & G_{\varphi x,x}(s) & G_{\varphi y,x}(s) \\ G_{x,y}(s) & G_{y,y}(s) & G_{z,y}(s) & G_{\varphi x,y}(s) & G_{\varphi y,y}(s) \\ G_{x,z}(s) & G_{y,z}(s) & G_{z,z}(s) & G_{\varphi x,z}(s) & G_{\varphi y,z}(s) \\ G_{x,\varphi x}(s) & G_{y,\varphi x}(s) & G_{z,\varphi x}(s) & G_{\varphi x,\varphi x}(s) & G_{\varphi y,\varphi y}(s) \\ G_{x,\varphi y}(s) & G_{y,\varphi y}(s) & G_{z,\varphi y}(s) & G_{\varphi x,\varphi y}(s) & G_{\varphi y,\varphi y}(s) \end{bmatrix} \cdot \begin{bmatrix} u_x(s) \\ u_y(s) \\ u_z(s) \\ u_{\varphi x}(s) \\ u_{\varphi y}(s) \end{bmatrix} \tag{3}$$

To examine the couplings between the entire axes, measurements of all transfer functions have been performed. The normalized static transfer values are given in Equation 4.

$$G_{norm}(s=0) = \begin{bmatrix} 1 & 0{,}0129 & 0{,}0231 & 0{,}0354 & 0{,}0508 \\ 0{,}0525 & 1 & 0{,}0480 & 0{,}1091 & 0{,}0308 \\ 0{,}0033 & 0{,}0021 & 1 & 0{,}0137 & 0{,}0174 \\ 0{,}0032 & 0{,}4214 & 0{,}0317 & 1 & 0{,}0214 \\ 0{,}8794 & 0{,}0050 & 0{,}0316 & 0{,}0239 & 1 \end{bmatrix} \tag{4}$$

It is obvious that there are two main couplings. First, a drive signal on the y-axis causes an unwanted output in φ_x-direction and second, an input signal in x-direction results in a displacement in φ_y-direction. The rest of the non-diagonal elements of the static transfer matrix are one or two orders of magnitude smaller. These values only have a marginal impact of the spindle supports transfer behaviour. By setting these marginal couplings to zero, the complete system can be described by the matrix given in Equation (5) or by the block diagram shown in Figure 5 right.

$$G(s) = \begin{bmatrix} G_{x,x}(s) & 0 & 0 & 0 & 0 \\ 0 & G_{y,y}(s) & 0 & 0 & 0 \\ 0 & 0 & G_{z,z}(s) & 0 & 0 \\ 0 & G_{y,\varphi x}(s) & 0 & G_{\varphi x,\varphi x}(s) & 0 \\ G_{x,\varphi y}(s) & 0 & 0 & 0 & G_{\varphi y,\varphi y}(s) \end{bmatrix} \tag{5}$$

3.2. Design of the decoupling network

The main objective in designing a decoupling network is to get a transfer behaviour that only depends on the input signal of the main transfer path. This can be achieved by adding an additional matrix between the controller output **V** and the amplifier input **U**, as shown in Figure 5. The transfer function matrix of this configuration is

$$\mathbf{Z}(s) = \mathbf{G}(s) \cdot \mathbf{D}(s) \cdot \mathbf{V}(s) \tag{6}$$

To obtain a completely decoupled behaviour Eq. 6 has to be equal to

$$\mathbf{Z}(s) = \mathbf{G}_D(s) \cdot \mathbf{V}(s) \tag{7}$$

$\mathbf{G}_D(s)$ is a diagonal matrix with the transfer functions of $G_{i,i}$ as elements as shown in Equation (8).

$$\mathbf{G}_D(s) = \begin{bmatrix} G_{x,x}(s) & 0 & 0 & 0 & 0 \\ 0 & G_{y,y}(s) & 0 & 0 & 0 \\ 0 & 0 & G_{z,z}(s) & 0 & 0 \\ 0 & 0 & 0 & G_{\varphi x,\varphi x}(s) & 0 \\ 0 & 0 & 0 & 0 & G_{\varphi y,\varphi y}(s) \end{bmatrix} \tag{8}$$

The conditions to reach the aspired behaviour can be calculated by a coefficient comparison given by

$$\mathbf{G}_D(s) = \mathbf{G}(s) \cdot \mathbf{D}(s) \tag{9}$$

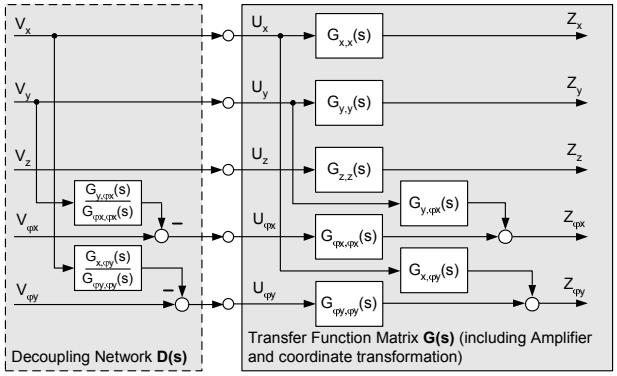

Figure 5: Block diagram of the plant with added decoupling network.

The known matrices are $\mathbf{G}_D$ and **G** and the aspired decoupling network is **D** which can be calculated by transposing equation (8) to

$$\mathbf{D}(s) = \mathbf{G}(s)^{-1} \cdot \mathbf{G}_D(s) \tag{10}$$

The inverse transfer function matrix $\mathbf{G}^{-1}$ exists if the determinant is not zero, which is usually the case. The decoupling transfer function matrix for the adaptive spindle support is given by

$$G(s) = \begin{bmatrix} \frac{1}{G_{x,x}(s)} & 0 & 0 & 0 & 0 \\ 0 & \frac{1}{G_{y,y}(s)} & 0 & 0 & 0 \\ 0 & 0 & \frac{1}{G_{z,z}(s)} & 0 & 0 \\ 0 & -\frac{G_{y,\varphi x}(s)}{G_{\varphi x,\varphi x}(s)} & 0 & \frac{1}{G_{\varphi x,\varphi x}(s)} & 0 \\ -\frac{G_{x,\varphi y}(s)}{G_{\varphi y,\varphi y}(s)} & 0 & 0 & 0 & \frac{1}{G_{\varphi y,\varphi y}(s)} \end{bmatrix} \tag{11}$$

The diagonal elements of the matrix consist of the inverse transfer functions $G_{i,i}$. For a complete inversion of the transfer functions it has to be assumed that the number of its zeros is equal to the number of its poles. However this is the case for the described system.

The comparison of the coupled and decoupled transfer behaviour of a tilting displacement around the φy-axis is shown in Figure 6. Apparently, the couplings resulting from the y-directed dynamics at 55Hz and 300Hz are almost completely erased.

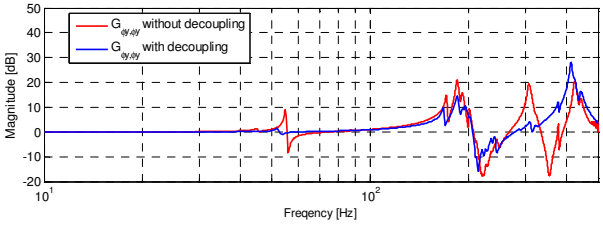

Figure 6: Measured FRF for a tilting displacement around φy-axis.

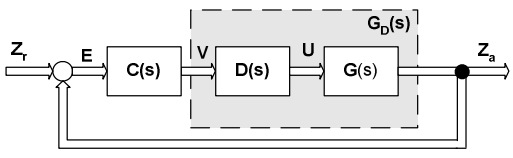

Figure 7: Structure of the feedback control.

With an implemented decoupling network it is possible to develop independent position controllers for every single Cartesian axis. A suitable approach for position control is the PID-controller. This approach is not model-based making it very robust against time variant differences in the transfer function. The algorithm can be described as

$$C_i(s) = k_i \cdot \frac{s^2 + a_i s + b_i}{s \cdot (s + c_i)} \tag{12}$$

The equation has a complex zero in the numerator that can be chosen in a way that it meets and compensates the first resonance of the correspondent axis. The parameter c_i describes the pole which is necessary for the practical realization. It can be optimised not to affect the dynamics of the axis. The proportional gain k_i is optimised at the test bench. The five PID-controllers can be concentrated in the controller matrix **C**. The simplified control scheme is shown in Figure 7.

4. System validation during cutting operation

4.1 Test setup

For tests the adaptive spindle support was mounted in the parallel kinematic test bench 3POD as shown in figures 1 and 8. The 3POD is able to move the spindle in three DOF (x, y, and z). The objective of the test was to produce a finish in line boring in a 40mm pre drilled aluminium block with a feed amount of 0.1 mm. The speciality of the borehole is a 4th order surface irregularity with an amount of ±50µm. Therefore the adaptive component carrying the spindle is moved in z-direction through the pre-drilled hole. Using a one-blade-cutter enables production of a surface parallel to the xy-plane with a constant geometry in z-direction. The reference values for the position control loop can be directly calculated from the given surface. Due to the two-dimensional irregularity of the surface, two sinusoidal functions for the x- and y-direction have to be determined. The frequency of these functions depends on the rotary speed of the spindle.

4.2. Results

To examine the performance of the spindle support and the controller, different measurements were done. First of all the kind of movement was determined. The described geometry can be created by moving the spindle translational in x- and y-direction or by tilting the spindle around x- and y- axes. Due to the mass of the spindle an operation in the translational mode was only possible up to 40Hz. For higher frequencies the performances of the actuators and amplifiers need to be increased. The same operation in tilting mode allows much higher frequencies. To examine the maximum operation frequency the measurements where repeated with increased spindle speed.

The resulting surface geometry was identified by using a coordinate measuring machine and compared with the reference geometry. Figure 8 shows the result for a spindle speed of 3.900 rpm. The measured cutting force was about 20N. The reachable maximum force was not determined yet.

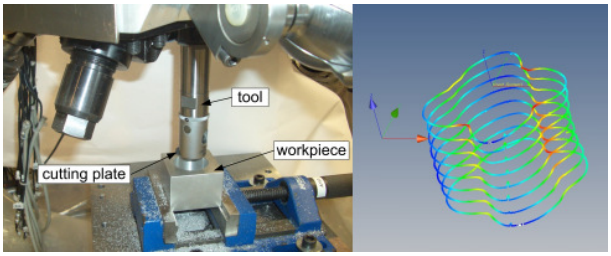

Figure 8: Experimental setup (left) measured surface geometry (right).

An operation frequency above 130Hz causes problems in the control loop due to the close resonance frequencies at 171Hz and above. The phase shift in the control loop increases over the critical value of 180 degrees and the control loop gets unstable. Lowering the proportional gain in the controller avoids that but also results in a lower bandwidth. The actual maximum operation frequency in tilting mode is therefore limited in this concept to approximately 130Hz.

5. Summary and outlook

The adaptive spindle support is a piezo-based drive design that is applicable for precision positioning in quasistatic and dynamic operations. Parallel kinematic drive designs cause the problem of static and dynamic couplings between the Cartesian axes. To examine these couplings a FE-Model of the adaptive spindle was created. The model considers the electromechanical behaviour of the piezoceramic actuators and is used to generate a state-space-model of the structure. It was validated by measuring the FRF between the actuators and the displacement of sensors at the spindle. The transfer behaviour was calculated from the measured FRF's numerical models. Based on that, a decoupling network was developed. That offered the possibility to design independent PID-position controllers for every Cartesian axis. The approach was tested during the in line boring process of an irregularity surface. According the measuring results a spindle movement frequency of 130Hz in tilting mode is possible. At this frequency the created surface is close to the given reference geometry. For the shown 4th order irregularity that means a maximum operation speed of 3900rpm.

Further research is focussed on increasing the operation frequency. Two aspects are of major interest. On one hand the performance of the actuators has to be increased while on the other hand the couplings of the solid state joint have to be reduced. This comes along with an optimisation of the single ball piezo connection joints, which are also a limiting factor. To deal with these tasks a new component using solid state joints for piezo connection will be designed. The couplings will be minimized during the design process by using the FE-calculated FRF as optimization criterion. The further aspect is to reduce the impact of the couplings by using more efficient control algorithms. An appropriate way is to add the decoupling network in actuator coordinates instead of adding it in Cartesian coordinates.

References

[1] Namazi, M. , Altintas, Y., Abe, T., Rajapakse, N., Modeling and identification of tool holder-spindle interface dynamics, 2007, J. o. Machine Tools & Manufacture, 47/9:1333-1341.

[2] Neugebauer, R.; Denkena, B.; Wegener, K., 2007, Mechatronic Systems for Machine Tools, Annals of the CIRP, 56/2.

[3] O'Neal, G.P.; Min, B-K.; Pasek, Z.J.; Koren, Y.,2001, Integrated Structural/Control, Design of Micro-Positioner for Boring Bar Tool Insert, J. o. Intelligent Material Systems and Structures, 12/Sept:617-627.

[4] Wittstock, V., 2007, Piezobasierte Aktor-Sensor-Einheiten zur uniaxialen Schwingungskompensation in Antriebssträngen von Werkzeugmaschinen, Verlag Wissenschaftliche Scripten, Zwickau.

[5] Drossel, W.-G.; Wittstock, V.: Adaptive Spindle Support for Improving Machining Operations. 58th General Assembly CIRP 2008, Manchester (UK), CIRP Annals 57 (2008) Nr.1, S.395-398

[6] Denkena, B.; Möhring, H.-C.; Will, J. C., 2005, Design and layout of an adaptronic spindle system, CIRP Journal of Manufacturing Systems, 34/3:247-257.

[7] Kranz, B., 2009, Zustandsraumbeschreibung von piezo-mechanischen Systemen auf Grundlage einer Finite-Elemente-Diskretisierung, ANSYS Conference & 27th CADFEM Users' Meeting, November 18-20, 2009 Congress Center Leipzig, Germany, pp 2.9.16